

Influence of the Atomic Structure on the Raman Spectra of Graphite Edges

L. G. Cançado,¹ M. A. Pimenta,¹ B. R. A. Neves,¹ M. S. S. Dantas,² and A. Jorio¹

¹*Departamento de Física, Universidade Federal de Minas Gerais, 30123-970, Belo Horizonte, Brazil*

²*Departamento de Engenharia Metalúrgica e de Materiais, Universidade Federal de Minas Gerais, 30160-030, Belo Horizonte, Brazil*

(Received 9 June 2004; published 7 December 2004)

A study of step edges in graphite with different atomic structures combining Raman spectroscopy and scanning probe microscopy is presented. The orientation of the carbon hexagons with respect to the edge axis, in the so-called armchair or zigzag arrangements, is distinguished spectroscopically by the intensity of a disorder-induced Raman peak. This effect is explained by applying the double resonance theory to a semi-infinite graphite crystal and by considering the one-dimensional character of the defect.

DOI: 10.1103/PhysRevLett.93.247401

PACS numbers: 78.30.Na, 78.66.Tr, 78.67.-n

The study of fundamental physical properties of graphite has increased in the last few years, since the discovery of new graphitelike carbon forms such as fullerenes and nanotubes [1]. In particular, the investigation of defects has become important with the fast development of graphite based nanostructures, such as nanotube devices presenting junctions, open ends, impurities, etc., and Raman spectroscopy is one of the main tools used for defect characterization. In this Letter, we present combined micro-Raman spectroscopy and scanning probe microscopy experiments showing that micro-Raman spectroscopy can be used to give information about the local arrangement of carbon atoms in a graphite edge. Specifically, unusual anisotropy in the Raman scattering is used to define the orientation of the carbon hexagons with respect to the graphite edge, in the so-called armchair or zigzag arrangements, as well as to define the local degree of order of the atomic structure at the edge. The physics leading to this structurally selective effect is explained on the basis of the well established double resonance effect [2,3] that is here applied to a semi-infinite crystal bounded by a one-dimensional defect.

Figure 1 shows three Raman spectra obtained at different regions of a highly oriented pyrolytic graphite (HOPG). The inset to Fig. 1 shows an optical image of the sample, obtained by a charge coupled device camera coupled to the microscope of the micro-Raman system. Regions 1 and 2 are at HOPG edges, while region 3 is on the flat HOPG surface. In all spectra, the light propagation is perpendicular to the HOPG basal plane and the polarization of the incident light is parallel to the edge direction in spectra 1 and 2. The Raman active E_{2g_2} vibrational mode of graphite gives rise to the so-called G band, which is centered at approximately 1580 cm^{-1} [4]. It is present in all spectra with the same intensity. The Raman features at approximately 1340 and 1620 cm^{-1} are disorder-induced bands that are observed in defective graphite structures, called D and D' bands, respectively. The mechanism giving rise to these bands is the double

resonance process, well established and largely used to explain the existence of disorder-induced peaks in the Raman spectra of several graphitelike materials, such as graphite fibers and carbon nanotubes [2,3].

The disorder-induced D and D' bands are observed in spectra 1 and 2, but not in spectrum 3. Spectrum 3 was taken in a flat region of the HOPG sample with a perfect crystalline order (see Fig. 1). The edge, on other hand, behaves as a defect necessary for momentum conservation in the double resonance Raman process. However, the most striking result shown in Fig. 1 is the fact that the D band is about 4 times less intense in spectrum 2 compared to spectrum 1, whereas the D' band intensity remains almost constant in both spectra. The different

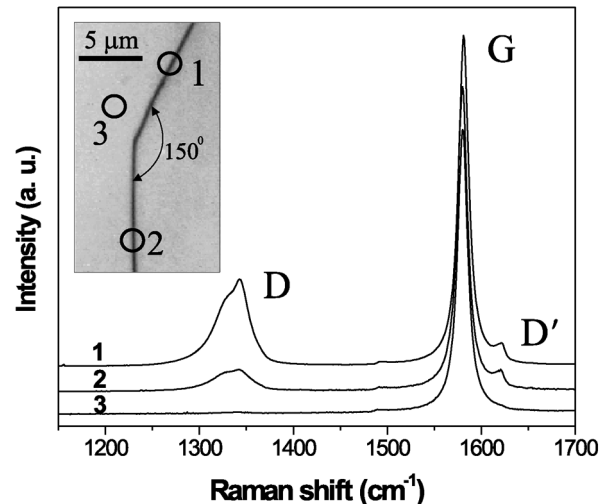


FIG. 1. Raman spectra obtained in three different regions of the HOPG sample. The spectra were taken at room temperature using a JY Horiba LabRam 800 monochromator system. The laser power density on the sample was $3 \times 10^5\text{ W/cm}^2$ and the laser energy was 1.96 eV. The inset shows an optical image of the step and the regions where spectra 1, 2, and 3 were taken (open circles).

intensities observed for the *D* band in spectra **1** and **2** indicate an intrinsic structural property of the scattering process in graphite edges.

To structurally characterize the sample, scanning probe microscopy measurements were performed using a Nanoscope IV MultiMode microscope from Veeco Instruments. Atomic force microscopy (AFM) data were obtained in the intermittent contact mode, at room temperature, using standard Si cantilevers. Figure 2(a) shows an AFM image of the step on the HOPG substrate where the Raman measurements in Fig. 1 were performed. The step is composed of two edges, forming an angle of 150° . The step height is about 230 nm, which corresponds to ~ 700 graphene sheets. The spikes along the edges [see the white arrow in Fig. 2(a)] are probably caused by agglutination of dust deposited on the HOPG surface due to laser heating. Figure 2(b) shows another AFM image of the edge **2** and scanning tunneling microscopy (STM) measurements were performed in the region marked by the white **X** in Fig. 2(b). The raw STM data [Fig. 2(c)] exhibit atomic spacing resolution, allowing a structural analysis of the edges. Figure 2(d) shows a fast Fourier transform (FFT)-filtered zoom image of the region marked by a white square in Fig. 2(c). There are two inequivalent atoms in the graphite unit cell, **A** and **B**, and STM measurements performed in the basal plane of graphite are normally able to distinguish one of them (**B** atoms) [5], which correspond to the dark regions in Fig. 2(d). The positions of **A** atoms are also indicated by small black squares in Fig. 2(d). A zigzag line connects **A** and **B** neighbor atoms and, following the white dashed line in Fig. 2, it can be concluded that edge **2** has a zigzag structure. Therefore, edge **1** must have an armchair struc-

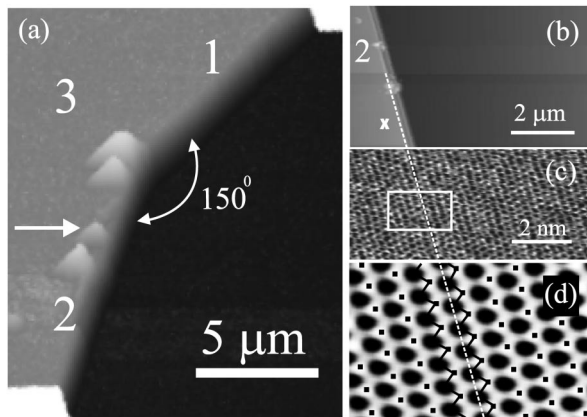


FIG. 2. (a) AFM image of the step on the HOPG substrate where Raman spectra shown in Fig. 1 were taken. (b) AFM image of edge **2**. (c) Atomic resolution STM image of the region marked by the white **X** in (b). The STM measurements were performed under ambient conditions in the constant-height mode. (d) FFT filtered image from the region marked by a white square in (c).

ture since, as shown in Figs. 1 and 2(a), edges **1** and **2** form an angle of 150° to each other [see Fig. 3(b)].

Knowing the edge structures, the Raman scattering events shown in Fig. 1 can be discussed. Figure 3(a) shows one possible intervalley double resonance process that gives rise to the *D* band in the Stokes spectra of disordered graphite materials [3,6]. This process begins with an electron of wave vector \vec{k} (measured from the *K* point) absorbing a photon of energy E_{laser} . Since the electronic energy dispersion of graphite is symmetric around the *K* point, the set of all electron wave vectors that can participate in this resonant absorption process forms a circle centered at the *K* point, with radius $|\vec{k}|$ (neglecting the trigonal warping effect [1]). The electron is inelastically scattered by a phonon of wave vector \vec{q} and energy E_{phonon} to a point belonging to a circle around the *K'* point, with radius $|\vec{k}'|$. After that, the electron is scattered back to \vec{k} by a defect with wave vector $\vec{d} = -\vec{q}$ and, finally, the electron-hole recombination occurs at \vec{k} , giving rise to the scattered photon with energy $E_{\text{laser}} - E_{\text{phonon}}$. This double resonance mechanism is called an intervalley process because it connects points in circles

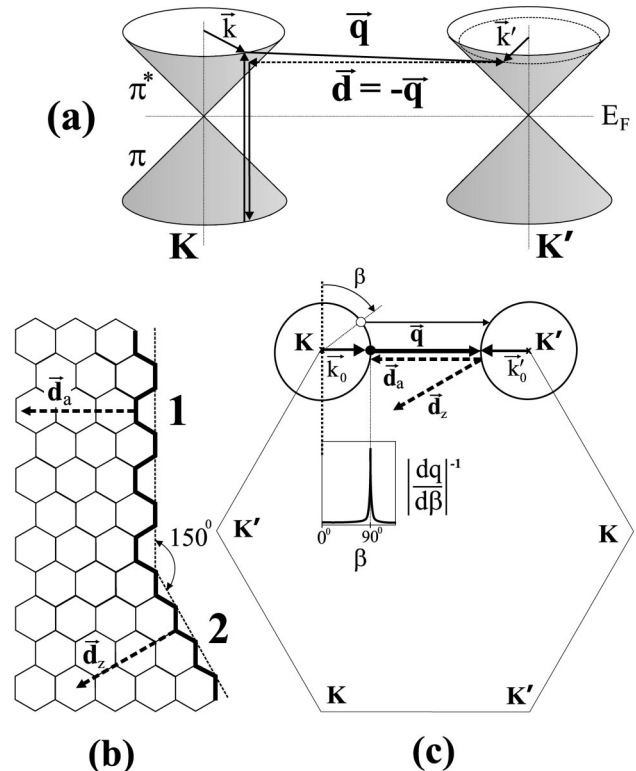


FIG. 3. (a) Representation of a double resonance Raman process that gives rise to the *D* band in the Stokes spectra of disordered graphite materials [3,6]. (b) Schematic illustration of the atomic structure of the step shown in Figs. 1 and 2. (c) First Brillouin zone of 2D graphite, showing the double resonant mechanism for an armchair graphite edge and the density of phonons (inset) associated with this process.

around inequivalent K and K' points in the first Brillouin zone of 2D graphite. On the other hand, the double resonance process that originates the D' band is an intravalley process [not shown in Fig. 3(a)], since it connects two points belonging to the same circle around the K point (or the K' point) [3].

The most common case of disorder-induced bands in the Raman spectra of graphite-related materials occurs in samples formed by aggregates of small crystallites. In this case, the crystallite borders form defects in the real space. Since the crystallites have different sizes and their boundaries are randomly oriented, the defect wave vectors exhibit all possible directions and values. Therefore, the existence of a defect with momentum exactly opposite to the phonon momentum is always possible, giving rise to double resonance processes connecting any pair of points in the circles around the K and K' points. In this case, the intensity of the D band is isotropic and does not depend on the light polarization direction. However, in the case of edges, the D band intensity is anisotropic because the double resonance process cannot occur for any pair of points. Since, in the real space, the edge defect is well localized in the direction perpendicular to the edge, it is completely delocalized in this direction in the reciprocal space and, therefore, the wave vector of such a defect assumes all possible values perpendicular to the step edge. Hence, the defect associated with a step edge has a one-dimensional character and it is only able to transfer momentum in the direction perpendicular to the edge.

Figure 3(b) shows the structure of the two kinds of edges shown in Figs. 1 and 2(a). The bold lines show the edge structures, armchair for edge **1** and zigzag for edge **2**. The wave vectors of the defects associated with these edges are represented by \vec{d}_a for armchair and \vec{d}_z for the zigzag edge. Figure 3(c) shows the first Brillouin zone of 2D graphite oriented according to the lattice in the real space shown in Fig. 3(b). Note that only the armchair \vec{d}_a vector is able to connect points belonging to circles centered at two inequivalent K and K' points. Considering the laser energy used in this work (2.54 eV), the radius of the circles around K' and K points is not large enough to allow the connection of any \vec{k}' and \vec{k} states by a zigzag \vec{d}_z vector. Therefore, the intervalley double resonance process associated with this defect cannot occur for a perfect zigzag edge. The mechanism depicted in Fig. 3(c) can thus explain the results shown in Fig. 1. The D band is much less intense in the spectra obtained in edge **2**, which has a zigzag structure.

It is also important to note the observation of a weak D band in spectrum **2**, where it should be absent. This weak D band is related to imperfections in the atomic structure of the edge, allowing the scattering of the electron by phonons and defects with wave vectors not perpendicular to the edge. Similar measurements performed on differ-

ent closely related armchair and zigzag graphite edges (similar to Fig. 2) show different D band intensity ratios, indicating different degrees of order for the local atomic arrangement at the different edges.

On the other hand, the D' band, around 1620 cm^{-1} , is given by an intravalley process, which connects points belonging to the same circle around the K (or K') point. In this case, momentum conservation can be satisfied by both \vec{d}_a and \vec{d}_z vectors and, therefore, the observation of the D' band must be independent on the edge structure. This conclusion is confirmed by the experimental result shown in Fig. 1, where the D' band has the same intensity in both spectra **1** and **2**, with armchair and zigzag structures, respectively.

The intervalley double resonance mechanism in armchair edges can now be discussed in details to fully characterize the one-dimensional character of the defect. The arrow starting from the open dot in Fig. 3(c) represents a possible phonon that can be associated with the D band in an armchair edge, since its wave vector has the same direction as \vec{d}_a . In principle, all phonons with wave vectors in this direction, connecting circles centered at K and K' , satisfy the double resonance condition. An important point to be analyzed is the density of such phonons, which is given by the relation $|dq/d\beta|^{-1} \propto |\sec\beta|$, where β is an arbitrary angle measured from the armchair edge direction [see Fig. 3(c)]. As shown in the inset of Fig. 3(c), the density of phonons exhibits a singularity for $\beta = 90^\circ$. Thus, it can be concluded that the D band is mainly associated with the phonon represented by the bold arrow starting from the black dot in Fig. 3(c), connecting the electronic states whose wave vectors \vec{k}_0 and \vec{k}'_0 have the same direction as \vec{d}_a .

Figure 4 shows the dependence of the D band intensity on the polarization of both incident and scattered light. The spectra were obtained at the armchair edge (edge **1**), and θ is the angle between the polarization vector of incident light and the edge direction (see the inset of Fig. 4). For spectra obtained in VV (VH) configuration, the scattered light was analyzed parallel (perpendicular) to the polarization direction of the incident light (V and H denote vertical and horizontal polarizations, respectively). As shown in Fig. 4, the D band intensity in VV configuration [$I_D(VV)$] decreases gradually with an increasing value of θ (filled squares), while in VH configuration, $I_D(VH)$ exhibits a maximum value for $\theta = 45^\circ$ (open squares).

In order to explain these results, it is first necessary to consider the polarization dependence of the optical transitions in graphite. Theoretical calculations predicted the anisotropy in the optical absorption (emission) coefficient of 2D graphite given by [7]

$$W_{\text{abs,ems}} \propto |\vec{P} \times \vec{k}|^2, \quad (1)$$

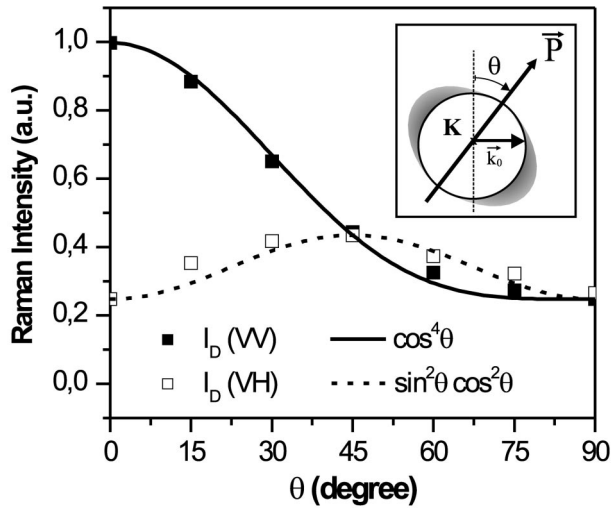


FIG. 4. (a) Dependence of the D band intensity on the polarization direction of incident and scattered light. The spectra were taken in region **1** (armchair edge) at room temperature using a Dilor XY triple-monochromator system. The laser power density on the sample was 3×10^5 W/cm² and the laser energy was 2.41 eV. The inset shows a schematic illustration of the optical anisotropy around the K point of 2D graphite, where θ is the angle between light polarization \vec{P} and the armchair edge direction.

where \vec{P} is the polarization of the incident (scattered) light for the absorption (emission) process, and \vec{k} is the wave vector of the electron measured from the K point. The thickness of the gray region around the circle shown in the inset to Fig. 4 illustrates the anisotropy in the optical absorption relative to \vec{P} , given by Eq. (1). Note that the light absorption (emission) has a maximum for electrons with wave vector \vec{k} perpendicular to \vec{P} , and it is null for electrons with wave vector parallel to \vec{P} . For the mechanism discussed in Fig. 3(c), the existence of a singularity in the density of phonons that participate in the one-dimensional double resonance intervalley process restricts the wave vector \vec{k} of the electron to the direction perpendicular to the armchair edge ($\vec{k} = \vec{k}_0$). In the VV configuration, \vec{P} has the same direction for the incident and scattered light, and since \vec{k}_0 is perpendicular to the armchair edge direction, the coefficients of absorption W_{abs} and emission W_{ems} are both proportional to $\cos^2\theta$. In VH configuration, the polarizations of the incident and scattered light are perpendicular to each other and, therefore, W_{abs} and W_{ems} are proportional to $\cos^2\theta$ and $\sin^2\theta$, respectively. Since the Raman scattering involves absorption and emission of photons, the D band intensity de-

picted in Fig. 4(a) is expected to be given by $I_D(VV) \propto \cos^4\theta$ and $I_D(VH) \propto \sin^2\theta\cos^2\theta$. The fit of the experimental data according to these expressions are also shown in Fig. 4(a), where solid and dashed lines are the curves obtained for $I_D(VV)$ and $I_D(VH)$, respectively. It is interesting to observe in Fig. 4(a) that the minimum values obtained for both $I_D(VV)$ and $I_D(VH)$ are not zero but correspond in fact to the D band intensity in the Raman spectrum of the zigzag edge **2** (see Fig. 1). In this way, the angular dependence of $I_D(VV)$ and $I_D(VH)$ have been fit considering an intensity background which is related to the double resonance Raman process associated with imperfections in the edge structure, which also contributes to the D band intensity. As pointed out earlier, the intensity background is different for different graphite edges, giving a measure of the local order of the C atom arrangement at the different edges. Furthermore, similar measurements on the zigzag edges show that the polarization dependence of the weak D band in spectrum **2** is anisotropic, with minimum intensity when the light polarization is perpendicular to the armchair edge.

In summary, this Letter presents a detailed study of graphite edges with different atomic structures, combining the use of Raman spectroscopy and scanning probe microscopy. This one-dimensional defect selects the direction of the electron and phonon associated with the disorder-induced Raman process and causes a dependence of the Raman D band intensity on the atomic structure of the edge (strong for armchair and weak for zigzag edge). This work, therefore, represents an effort to improve the understanding of the influence of the defect structure on the Raman spectra of graphitelike systems, which may be very useful to characterize defects in nanographite-based devices.

This work is supported by Instituto de Nanociências and FAPEMIG, Brazil. L. G. C. acknowledges support from the Brazilian Agencies CAPES and CNPq.

-
- [1] R. Saito *et al.*, *Physical Properties of Carbon Nanotubes* (Imperial College Press, London, 1998).
 - [2] C. Thomsen and S. Reich, *Phys. Rev. Lett.* **85**, 5214 (2000).
 - [3] R. Saito *et al.*, *Phys. Rev. Lett.* **88**, 027401 (2002).
 - [4] F. Tuinstra and J. L. Koenig, *J. Chem. Phys.* **53**, 1126 (1970).
 - [5] I. P. Batra and S. Ciraci, *J. Vac. Sci. Technol. A* **6**, 313 (1988).
 - [6] L. G. Cançado *et al.*, *Phys. Rev. B* **66**, 035415 (2002).
 - [7] A. Gruneis *et al.*, *Phys. Rev. B* **67**, 165402 (2003).